

Spitzer Identification of the Least Massive Known Brown Dwarf with a Circumstellar Disk

K. L. Luhman¹, Paola D'Alessio², Nuria Calvet¹, Lori E. Allen¹, Lee Hartmann¹, S. T. Megeath¹, P. C. Myers¹, & G. G. Fazio¹

ABSTRACT

Using the Infrared Array Camera (IRAC) aboard the *Spitzer Space Telescope*, we have obtained mid-infrared photometry of the least massive known brown dwarf in the Chamaeleon I star-forming region. For this young brown dwarf, OTS 44, we have constructed a spectral energy distribution (SED) from 0.8–8 μm by combining the measurements at 3.6, 4.5, 5.8, and 8.0 μm from IRAC with ground-based photometry at *I*, *J*, *H*, and *K*. The resulting SED for OTS 44 exhibits significant excess emission longward of 3 μm relative to the SED expected from the photosphere of the brown dwarf. We have successfully modeled the source of this excess emission in terms of an irradiated viscous accretion disk with $\dot{M} \lesssim 10^{-10} M_{\odot} \text{yr}^{-1}$. With a spectral type of M9.5 and a mass of $\sim 15 M_{\text{Jup}}$, OTS 44 is now the coolest and least massive brown dwarf observed to have a circumstellar disk. These measurements demonstrate that disks exist around brown dwarfs even down to the deuterium burning mass limit and the approximate upper mass limit of extrasolar planetary companions.

Subject headings: accretion disks – planetary systems: protoplanetary disks – stars: formation — stars: low-mass, brown dwarfs — stars: pre-main sequence

1. Introduction

Measuring the lowest mass at which brown dwarfs harbor circumstellar disks is crucial for understanding the formation mechanism of brown dwarfs and for determining whether planets can form around low-mass brown dwarfs. The natural laboratories for performing

¹Harvard-Smithsonian Center for Astrophysics, 60 Garden St., Cambridge, MA 02138; kluhman, ncalvet, leallen, lhartmann, tmegeath, pmyers, gfazio@cfa.harvard.edu.

²Centro de Radiostaronomía y de Astrofísica, UNAM, Apartado Postal 72-3 (Xangari), 58089 Morelia, Michoacán, México; p.dalessio@astrosmo.unam.mx

this measurement are the nearest regions of star formation ($\tau \sim 0.5\text{-}3$ Myr, $d = 150\text{-}300$ pc), particularly those that have been surveyed extensively for brown dwarfs (e.g., Luhman 1999; Comerón et al. 2000; Martín et al. 2001; Briceño et al. 2002). For some of the young brown dwarfs discovered in these surveys¹, indirect evidence of circumstellar disks has been obtained through detections of accretion. The most readily observed signature of accretion in a young brown dwarf is a broad H α emission line profile, which has been observed through high-resolution spectroscopy in GM Tau, IC 348-382, and IC 348-415 at a spectral type of M6.5 (White & Basri 2003; Muzerolle et al. 2003) and in IC348-355 and 2MASS 1207-3932 at M8 (Jayawardhana et al. 2003b; Mohanty et al. 2003). Very large equivalent widths of H α in low-resolution spectra also have been suggestive of accretion in KPNO-Tau 12 and S Ori 55 at M9 (Luhman et al. 2003a; Zapatero Osorio et al. 2002) and in S Ori 71 at L0 (Barrado y Navascués et al. 2002). High-resolution data has confirmed the presence of accretion in KPNO-Tau 12, as well as in several other young sources at M6.25-M8.5 (Muzerolle et al. 2005; Mohanty et al. 2005).

Direct evidence of circumstellar disks around brown dwarfs has been provided by detections of infrared (IR) emission above that expected from stellar photospheres alone. Modest excess emission in the K and L bands has been observed for several young objects at M6-M8 and for a few as late as M8.5 (Luhman 1999, 2004; Lada et al. 2000, 2004; Muench et al. 2001; Liu et al. 2003; Jayawardhana et al. 2003a). At longer, mid-IR wavelengths, the *Infrared Space Observatory (ISO)* detected excesses for CFHT 4 at M7 (Pascucci et al. 2003), Cha H α 1 at M7.75 (Persi et al. 2000; Comerón et al. 2000; Natta & Testi 2001b), and GY141 at M8.5 (Comerón et al. 1998). Photometry at similar wavelengths was recently obtained from the ground with Gemini Observatory for CFHT 4 (Apai et al. 2004), Cha H α 1, and 2MASS 1207-3932 (Sterzik et al. 2004). Detections of circumstellar material around young brown dwarfs have been extended to millimeter wavelengths for CFHT 4, as well as for IC 348-613 at M8.25 (Klein et al. 2003). Additional detections of accretion and disks have been reported for objects in Ophiuchus with IR spectral types of M6 and later (Testi et al. 2002; Natta et al. 2002, 2004; Mohanty et al. 2004). However, because those types were derived from water absorption bands by using field M dwarfs as the standards, they likely have systematic errors such that the temperatures, and thus the masses, are underestimated (Luhman et al. 2003b, 2004).

To continue to search for circumstellar disks around brown dwarfs at later types and lower masses, we have obtained mid-IR photometry with the Infrared Array Camera (IRAC;

¹The hydrogen burning mass limit at ages of 0.5-3 Myr corresponds to a spectral type of \sim M6.25 according to the models of Baraffe et al. (1998) and Chabrier et al. (2000) and the temperature scale of Luhman et al. (2003b).

Fazio et al. 2004) on the *Spitzer Space Telescope* for source 44 from Oasa et al. (1999) (hereafter OTS 44), which is the coolest and least massive known brown dwarf in the Chamaeleon I star-forming region (M9.5, $M \sim 15 M_{\text{Jup}}$; Luhman et al. 2004). In this letter, we describe these observations, construct a spectral energy distribution (SED) for OTS 44, measure its mid-IR excess emission, and compare this excess to our model predictions for emission from a circumstellar disk.

2. Observations

As a part of the Guaranteed Time Observations of the IRAC instrument team, we obtained images at 3.6, 4.5, 5.8, and 8.0 μm with IRAC on the *Spitzer Space Telescope* of the northern cluster in the Chamaeleon I star-forming region on 2004 July 4 (UT). The plate scale and field of view of IRAC are $1''.2$ and $5'.2 \times 5'.2$, respectively. The camera produces images with FWHM = $1''.6$ – $1''.9$ from 3.6 to 8.0 μm (Fazio et al. 2004). The cluster was mapped with a 6×7 mosaic of pointings separated by $280''$ and aligned with the array axes. At each cell in the map, images were obtained in the 12 s high dynamic range mode, which provided one 0.4 s exposure and one 10.4 s exposure. The map was performed twice with offsets of several arcseconds between the two iterations. The resulting maps had centers of $\alpha = 11^{\text{h}}09^{\text{m}}26^{\text{s}}$, $\delta = -76^{\circ}36'26''$ (J2000) for 3.6 and 5.8 μm and at $\alpha = 11^{\text{h}}10^{\text{m}}16^{\text{s}}$, $\delta = -76^{\circ}30'20''$ (J2000) for 4.5 and 8.0 μm , dimensions of $33' \times 29'$, and position angles of 28° for the long axes. The images from the Spitzer Science Center pipeline (version S10.5.0) were combined into one mosaic at each of the four bands using custom IDL software developed by Robert Gutermuth.

Aperture photometry for OTS 44 was extracted with the task PHOT under the IRAF package APPHOT using a radius of two pixels ($2''.4$) for the aperture and inner and outer radii of two and six pixels for the sky annulus. In the next section, we will compare the IRAC measurements of OTS 44 to those of KPNO-Tau 4, a young brown dwarf in Taurus with the same spectral type as OTS 44. Therefore, we also measured KPNO-Tau 4 from images obtained by Hartmann et al. (2005) with the same aperture sizes applied to OTS 44. Because the 8.0 μm images of KPNO-Tau 4 were contaminated by residual images from a prior observation of a bright star, the photometry in this band is uncertain and therefore is not considered in this work. For an aperture radius of 10 pixels and a sky annulus extending from 10 to 20 pixels, we adopted zero point magnitudes (ZP) of 19.601, 18.942, 16.882, 17.395 in the 3.6, 4.5, 5.8 and 8 μm bands, where $M = -2.5 \log(DN/sec) + ZP$. We then applied aperture corrections of 0.210, 0.228, 0.349, and 0.499 mag to the photometry of OTS 44 and KPNO-Tau 4. The resulting IRAC photometry for OTS 44 and KPNO-Tau 4

are listed in Table 1. The photometric uncertainties for both objects are 0.02 mag at 3.6 and 4.5 μm and 0.04 mag at 5.8 and 8.0 μm , with an additional 10% uncertainty in the IRAC calibration. Table 1 includes optical and near-IR photometry for OTS 44 and KPNO-Tau 4. The data at I are from K. Luhman (in preparation) and Briceño et al. (2002) and the near-IR measurements are from Oasa et al. (1999) and the 2MASS Point Source Catalog for OTS 44 and KPNO-Tau 4, respectively.

3. Analysis

Before discussing OTS 44, we first examine the SED of the comparison source, KPNO-Tau 4. Figure 1 shows the SED of KPNO-Tau 4 derived from the photometry in Table 1 using a distance modulus of 5.76 for Taurus (Wichmann et al. 1998) and the appropriate zero-magnitude fluxes (Bessell 1979; Bessell & Brett 1988; Fazio et al. 2004). No correction for extinction was applied to these data because of the negligible extinction toward this object (Briceño et al. 2002). As shown in Figure 1, the mid-IR SED of KPNO-Tau 4 is consistent with a blackbody at the effective temperature of the central object ($T_{\text{eff}} = 2300$ K; Luhman et al. 2004)², and thus exhibits no evidence of excess emission from circumstellar material. Therefore, in the following analysis, we adopt the SED of KPNO-Tau 4 to represent the intrinsic photosphere of young objects at the spectral type of OTS 44.

We now examine the SED of OTS 44, which is shown in Figure 1 after an extinction correction of $A_J = 0.3$ (Luhman et al. 2004) and adopting a distance modulus of 6.13 for Chamaeleon I (Whittet et al. 1997; Wichmann et al. 1998; Bertout et al. 1999). In comparison to KPNO-Tau 4, OTS 44 exhibits excess flux in the IRAC bands that becomes stronger with longer wavelengths. We have compared this excess emission with the predictions of a model of an irradiated accretion disk. For these calculations, we adopted a stellar mass $M_* = 0.015 M_\odot$ and radius $R_* = 0.23 R_\odot$ (Luhman et al. 2004), uniform grain size distribution everywhere given by the standard power law $n(a) \sim a^{-3.5}$ with minimum and maximum grain sizes $a_{\text{min}} = 0.005 \mu\text{m}$ and $a_{\text{max}} = 0.25 \mu\text{m}$ (Mathis, Rumpl, & Nordsieck 1977), uniform mass accretion rate, and an inner radius $R_{\text{in}} = 3 R_*$ (given by the silicate sublimation radius). The disk was heated by local viscous dissipation and stellar irradiation. The emission from a wall at the dust destruction radius was included. Detailed descriptions of the method used to calculate the disk structure and emergent intensity are given by D’Alessio et al. (1998), D’Alessio et al. (1999), and D’Alessio, Calvet, & Hartmann (2001).

²The mid-IR SED of an object at the age and temperature of KPNO-Tau 4 is predicted to agree with that of a blackbody (Allard et al. 2000).

As shown in Figure 1, we were able to fit the observed SED with a disk model seen pole-on ($i = 0$) with an accretion rate of $\dot{M} \sim 10^{-10} M_{\odot} \text{ yr}^{-1}$ and an inner radius of $3 R_{*}$. We were driven to low inclinations because we found that any significant contribution from the inner wall, which radiates approximately as a blackbody at 1400 K, resulted in an SED that was inconsistent with the IRAC observations. Our estimate of the accretion rate is higher than values derived for other young brown dwarfs from modeling of $\text{H}\alpha$ emission profiles (Muzerolle et al. 2003, 2005). Within the context of our model and the adopted inclination, we required substantial viscous dissipation due to accretion as well as irradiation from the central star to achieve high enough temperatures at the inner edge of the disk. Our model assumes that the inner disk wall is perfectly vertical (perpendicular to the disk plane). If the disk wall is actually somewhat tilted or curved, as was adopted to model the older T Tauri star TW Hya (Calvet et al. 2002), also seen pole-on, it is possible that the intermediate range of temperatures at the inner disk edge resulting from such structure would enable us to fit the observations with lower \dot{M} . Further exploration of this issue is needed.

The accretion luminosity for the adopted values of the stellar mass and radius and the disk mass accretion rate is $0.0002 L_{\odot}$, which corresponds to 15% of the stellar luminosity, $L_{*} = 0.0013 L_{\odot}$ (Luhman et al. 2004). If matter from the disk is loaded onto the star through a magnetospheric flow, as the observed line profiles in higher mass brown dwarfs and very low mass stars seem to indicate (Muzerolle et al. 2003, 2005; White & Basri 2003; Jayawardhana et al. 2003b; Mohanty et al. 2003, 2005), then an accretion shock should form at the stellar surface, where most of the accretion luminosity would be emitted (Calvet & Gullbring 1998; Gullbring et al. 2000). This emission would veil the photospheric lines. To estimate the expected degree of veiling, we have calculated the emission from accretion shocks on the stellar surface following the procedures of Calvet & Gullbring (1998). Figure 1 shows the shock emission from two models of accretion columns with values of the energy flux in the column $\mathcal{F} = 10^{11} \text{ erg cm}^{-2} \text{ s}^{-1}$ and $\mathcal{F} = 10^{12} \text{ erg cm}^{-2} \text{ s}^{-1}$, which are representative of those estimated for higher mass T Tauri stars (Calvet & Gullbring 1998) and correspond to filling factors on the stellar surface of 0.0016 and 0.00016, respectively. As shown in Figure 1, veiling from the shock is predicted to be significant at optical wavelengths but negligible longward of $1 \mu\text{m}$. Optical spectroscopy can test the model prediction of a high accretion rate; as discussed above, modifying the structure of the inner disk edge could result in acceptable fits with lower accretion rates and thus lower accretion shock luminosities.

The IRAC data do not constrain the maximum grain size. Disk models with different grain maximum sizes have the same SED for $\lambda < 9 \mu\text{m}$ because the fluxes arise from the optically thick and flat inner disk regions. Thus, observations at longer wavelengths are necessary for constraining the dust properties in the OTS 44 disk. Similarly, it is not possible to constrain the disk mass with the available data; models with a different viscosity parameter

α and disk radius (which implies different disk masses for a given mass accretion rate) have the same SED in the observed spectral range.

4. Discussion

Through observations with IRAC aboard the *Spitzer Space Telescope*, we have shown that the least massive known member of Chamaeleon I, OTS 44, exhibits strong mid-IR excess emission, which we have reproduced with a model of an accretion disk. With a spectral type of M9.5 and a mass of $\sim 15 M_{\text{Jup}}$, OTS 44 is now the coolest and least massive brown dwarf observed to have a circumstellar disk. The presence of a disk around OTS 44 demonstrates that the formation of free-floating bodies via disks extends down to the deuterium burning mass limit ($M \approx 14 M_{\text{Jup}}$; Burrows et al. 1997), and raises the possibility of planet formation around objects that themselves have planetary masses. Indeed, a candidate planetary companion has already been discovered near the earlier and more massive young brown dwarf 2MASS 1207-3932 (M8, $M \sim 30 M_{\text{Jup}}$; Gizis 2002) by Chauvin et al. (2004).

The relative ease of the detection of the excess emission from OTS 44 ($\tau_{\text{int}} = 20.8$ s) demonstrates the feasibility of searching for disks around young brown dwarfs at even lower masses with IRAC ($M < 10 M_{\text{Jup}}$). In addition, photometry at longer wavelengths with the Multiband Imaging Photometer for *Spitzer* and spectroscopy with the Infrared Spectrograph on *Spitzer* of OTS 44 and brown dwarfs like it should provide detailed constraints on the physical properties of disks around low-mass brown dwarfs, such as their mineralogy and geometry (e.g., Apai et al. 2004; Furlan et al. 2005).

We are grateful to Robert Gutermuth for developing the software used in reducing the IRAC images. K. L. was supported by grant NAG5-11627 from the NASA Long-Term Space Astrophysics program. P. D. acknowledges grants from CONACyT and PAPIIT/DGAPA, México. N. C. and L. H. acknowledge grant NAG5-13210. This work is based on observations made with the *Spitzer Space Telescope*, which is operated by the Jet Propulsion Laboratory, California Institute of Technology under NASA contract 1407. Support for this work was provided by NASA through contract 1256790 issued by JPL/Caltech. Support for the IRAC instrument was provided by NASA through contract 960541 issued by JPL. This publication makes use of data products from the Two Micron All Sky Survey, which is a joint project of the University of Massachusetts and the Infrared Processing and Analysis Center/California Institute of Technology, funded by the National Aeronautics and Space Administration and the National Science Foundation.

REFERENCES

- Apai, D., Pascucci, I., Sterzik, M. F., van der Blik, N., Bouwman, J., Dullemond, C. P., & Henning, Th. 2004, *A&A*, 426, L53
- Allard, F., Hauschildt, P. H., & Schweitzer, A. 2000, *ApJ*, 539, 366
- Baraffe, I., Chabrier, G., Allard, F., & Hauschildt, P. H. 1998, *A&A*, 337, 403
- Barrado y Navascués, D., Zapatero Osorio, M. R., Martín, E. L., Béjar, V. J. S., Rebolo, R., & Mundt, R. 2002, *A&A*, 393, L85
- Bertout, C., Robichon, N., & Arenou, F. 1999, *A&A*, 352, 574
- Bessell, M. S. 1979, *PASP*, 91, 589
- Bessell, M. S., & Brett, J. M. 1988, *PASP*, 100, 1134
- Briceño, C., Luhman, K. L., Hartmann, L., Stauffer, J. R., & Kirkpatrick, J. D. 2002, *ApJ*, 580, 317
- Burrows, A., et al. 1997, *ApJ*, 491, 856
- Calvet, N., D’Alessio, P., Hartmann, L., Wilner, D., Walsh, A., & Sitko, M. 2002, *ApJ*, 568, 1008
- Calvet, N., & Gullbring, E., 1998, *ApJ*, 509, 802
- Chabrier, G., Baraffe, I., Allard, F., & Hauschildt, P. H. 2000, *ApJ*, 542, 464
- Chauvin, G., et al. 2004, *A&A*, 425, L29
- Comerón, F., Rieke, G. H., Claes, P., Torra, J., & Laureijs, R. J. 1998, *A&A*, 335, 522
- Comerón, F., Neuhauser, R., & Kaas, A. A. 2000, *A&A*, 359, 269
- D’Alessio, P., Canto, J., Calvet, N., & Lizano, S. 1998, *ApJ*, 500, 411
- D’Alessio, P., Calvet, N., Hartmann, L., Lizano, S., & Cantó, J. 1999, *ApJ*, 527, 893
- D’Alessio, P., Calvet, N., & Hartmann, L. 2001, *ApJ*, 553, 321
- Fazio, G. G., et al. 2004, *ApJS*, 154, 10
- Furlan, E., et al. 2005, *ApJ*, submitted

- Gizis, J. E. 2002, *ApJ*, 575, 484
- Gullbring, E., Calvet, N., Muzerolle, J., & Hartmann, L. 2000, *ApJ*, 544, 927
- Hartmann, L., et al. 2005, *ApJ*, submitted
- Jayawardhana, R., Ardila, D. R., Stelzer, B., & Haisch, K. E. 2003a, *AJ*, 126, 1515
- Jayawardhana, R., Mohanty, S., & Basri, G. 2003b, *ApJ*, 592, 282
- Klein, R., Apai, D., Pascucci, I., Henning, Th., Waters, L. B. F. M. 2003, *ApJ*, 593, L57
- Lada, C. J., Muench, A. A., Haisch, K. E., Lada, E. A., Alves, J. F., Tollestrup, E. V., & Willner, S. P. 2000, *AJ*, 120, 3162
- Lada, C. J., Muench, A. A., Lada, E. A., & Alves, J. F. 2004, *AJ*, 128, 1254
- Liu, M. C., Najita, J., & Tokunaga, A. T. 2003, *ApJ*, 585, 372
- Luhman, K. L. 1999, *ApJ*, 525, 466
- Luhman, K. L. 2004, *ApJ*, 617, 1216
- Luhman, K. L., Briceño, C., Stauffer, J. R., Hartmann, L., Barrado y Navascués, D., & Nelson, C. 2003a, *ApJ*, 590, 348
- Luhman, K. L., Peterson, D. E., & Megeath, S. T. 2004, *ApJ*, 617, 565
- Luhman, K. L., Stauffer, J. R., Muench, A. A., Rieke, G. H., Lada, E. A., Bouvier, J., & Lada, C. J. 2003b, *ApJ*, 593, 1093
- Martín, E. L., Dougados, C., Magnier, E., Ménard, F., Magazzù, A., Cuilandre, J.-C., & Delfosse, X. 2001, *ApJ*, 561, L195
- Mathis, J. S., Rumpl, W., & Nordsieck, K. H. 1977, *ApJ*, 217, 425
- Mohanty, S., Jayawardhana, R., & Barrado y Navascués, D. 2003, *ApJ*, 593, L109
- Mohanty, S., Jayawardhana, R., Natta, A., Fujiyoshi, T., Tamura, M., & Barrado y Navascués, D. 2004, *ApJ*, 609, L33
- Mohanty, S., Jayawardhana, R., & Basri, G. 2005, *ApJ*, submitted
- Muench, A. A., Alves, J., Lada, C. J., & Lada, E. A. 2001, *ApJ*, 558, L51
- Muzerolle, J., Hillenbrand, L., Calvet, N., Briceño, C., & Hartmann, L. 2003, *ApJ*, 592, 266

- Muzerolle, J., Luhman, K. L., Briceño, C., Hartmann, L., & Calvet, N. 2005, *ApJ*, submitted
- Natta, A., & Testi, L. 2001, *A&A*, 376, L22
- Natta, A., Testi, L., Muzerolle, J., Randich, S., Comerón, F., & Persi, P. 2004, *A&A*, 424, 603
- Natta, A., et al. 2002, *A&A*, 393, 597
- Oasa, Y., Tamura, M., & Sugitani, K. 1999, *ApJ*, 526, 336
- Pascucci, I., Apai, D., Henning, Th., & Dullemond, C. P. 2003, *ApJ*, 590, L111
- Persi, P., et al. 2000, *A&A*, 357, 219
- Sterzik, M. F., Pascucci, I., Apai, D., van der Blik, N., & Dullemond, C. P. 2004, *A&A*, 427, 245
- Testi, L., et al. 2002, *ApJ*, 571, L155
- White, R. J., & Basri, G. 2003, *ApJ*, 582, 1109
- Whittet, D. C. B., Prusti, T., Franco, G. A. P., Gerakines, P. A., Kilkenny, D., Larson, K. A., & Wesselius, P. R. 1997, *A&A*, 327, 1194
- Wichmann, R., Bastian, U., Krautter, J., Jankovics, I., & Ruciński, S. M. 1998, *MNRAS*, 301, L39
- Zapatero Osorio, M. R., Béjar, V. J. S., Martín, E. L., Barrado y Navascués, D., & Rebolo, R. 2002, *ApJ*, 569, L99

Table 1. Photometry for OTS 44 and KPNO-Tau 4

ID	$I - J$	$J - H$	$H - K_s$	K_s	[3.6]	[3.6] – [4.5]	[4.5] – [5.8]	[5.8] – [8.0]
OTS 44	~ 4.7	1.01	0.79	14.61	13.67	0.41	0.53	0.70
KPNO-Tau 4	3.73	0.97	0.74	13.28	12.51	0.10	0.12	...

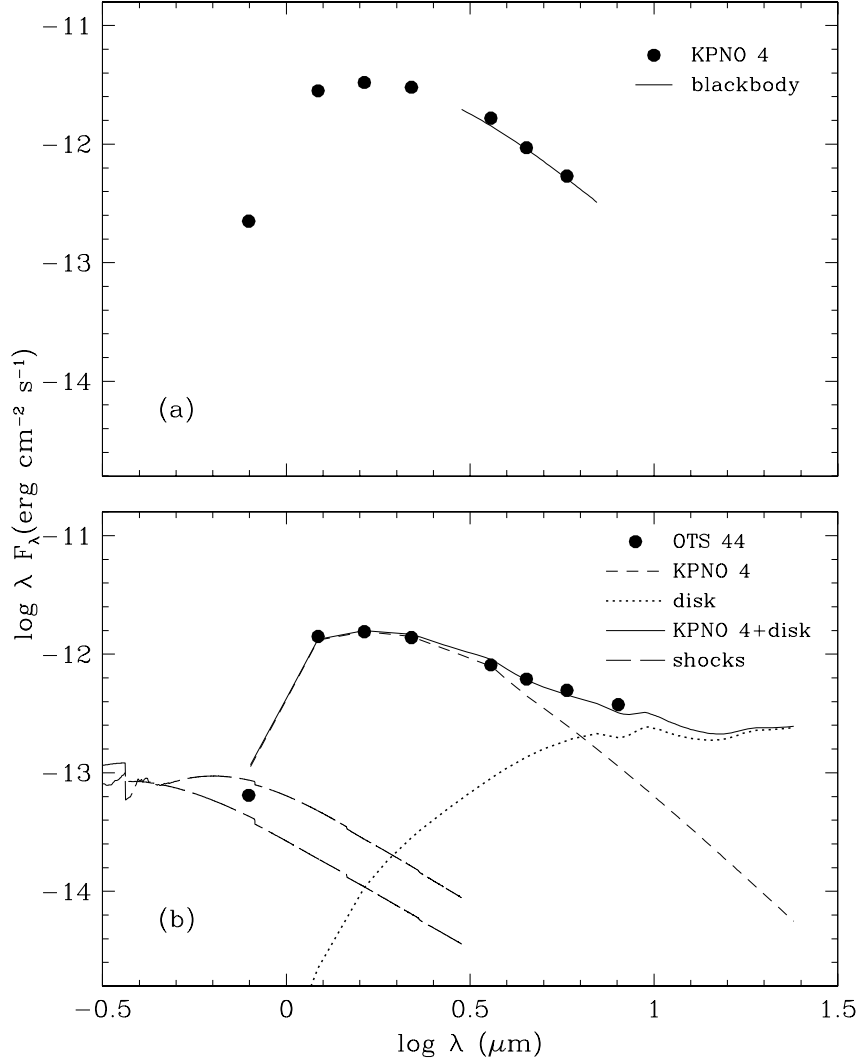


Fig. 1.— SEDs of the young brown dwarfs KPNO-Tau 4 and OTS 44 (*points*). (a) The slope of the mid-IR SED of KPNO-Tau 4 is reproduced by a blackbody at the effective temperature of its stellar photosphere ($T_{\text{eff}} = 2300 \text{ K}$, *solid line*), and thus exhibits no excess emission from circumstellar material. (b) To estimate the SED of the stellar photosphere of OTS 44, the measured SED of KPNO-Tau 4 is combined with the blackbody SED at $\lambda > 6 \mu\text{m}$ and scaled to the H -band flux of OTS 44 (*short dashed line*). The excess flux above this photospheric SED is modeled in terms of emission from a circumstellar accretion disk (*dotted line*). The sum of this model disk SED and the photospheric SED agrees fairly well with the data (*solid line*). The values of the model parameters are $\dot{M} = 10^{-10} \text{ M}_\odot \text{ yr}^{-1}$, an inclination angle to the line of sight $i = 0^\circ$ (i.e., pole-on), $\alpha = 0.01$, and $R_{\text{wall}} = 3 R_*$. We also include the SEDs predicted for the accretion shock for values of the energy flux that are representative of higher mass T Tauri stars, $\mathcal{F} = 10^{11}$ and $10^{12} \text{ erg cm}^{-2} \text{s}^{-1}$ (*long dashed lines*).